ATTITUDE DETERMINATION OF THE IMS ANTARCTIC SOUNDING ROCKETS

Fumio TOHYAMA and Iwao AOYAMA

Laboratory of Space Science, Tokai University, Kitakaname, Hiratsuka 259-12

Abstract: During the IMS period (1976–1978), 19 sounding rockets were launched at Syowa Station, Antarctica. 12 rockets of these were S-210 type vehicles and 7 rockets were S-310 type vehicles.

Vehicle attitudes have been determinated by use of geomagnetic aspect sensors and other aspect sensors. Most of the S-310 type vehicles took stable flight aspects with the average precession angle about 13 degrees and the period about 192 s. In the characteristics of S-210 type vehicle attitudes three kinds were distinguished; the first had aspects of small precession angles and long periods, the second had aspects of large precession angles and short periods, and the third had aspects of intermediate precession angles and periods. The average precession angle of S-210 type vehicles was about 32 degrees and the period was about 72 s.

1. Introduction

It is one of the most essential measurements to determine the attitude of a vehicle during the flight for the engineering of vehicle stabilities and analyses of physical observations.

The attitude is defined by the specification of three rotation angles, that are Eulerian, relating the vehicle axes to a known coordinate system. Most rockets are spun about its principal moment of inertia and the spin axis generally coincides with the longitudinal axis. One type of aspect sensor measures the angle between the spin axis and the external physical objects or fields, such as the sun, the earth or the geomagnetic field. If three different sensors give the tip angles, the orientation of the vehicle axis can be determined with an unambiguous solution. However, the use of only two different sensors is preferred, though it produces two-solution ambiguities, since one solution can be eliminated by physical arguments, and economy of space and cost is significant.

In Fig. 1, if the coordinates of the vector $\boldsymbol{P}$ and $\boldsymbol{Q}$ are known in a suitable coordinate system (X, Y, Z) and two sensor angles, α_p and α_q are measured that are angles between $\boldsymbol{R}$ and $\boldsymbol{P}$, and $\boldsymbol{R}$ and $\boldsymbol{Q}$ respectively, the possible orientations of the vehicle axis, $\boldsymbol{R}$ are at the points of intersection of two cones tracing out the circles of radii α_p and α_q on the celestial sphere. In general, the direction of $\boldsymbol{R}$ is at two points, $\boldsymbol{R}_1$ and $\boldsymbol{R}_2$. The methods to eliminate one solution are considered by pursuing the past history of the solutions from launch or by measuring angular phase Ψ_{qp} between

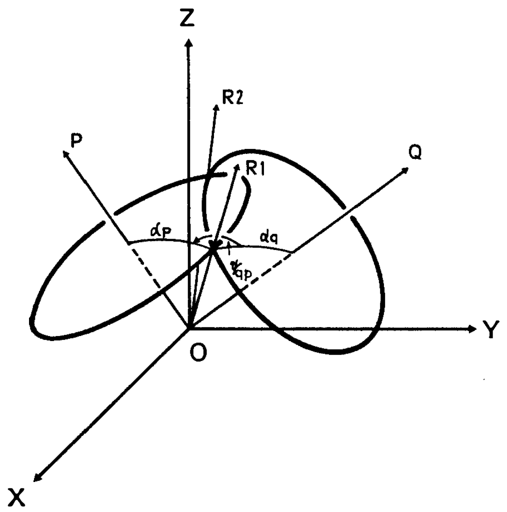

Fig. 1. Two cone intersection method. ***P*** *and* ***Q*** *are given vectors of external physical objects or fields in the inertia coordinate system.* α_p *and* α_q *are sensor angles that are measured from aspect sensors, and two solutions* $\boldsymbol{R}_1$ *or* $\boldsymbol{R}_2$ *may be the orientation of the rocket axis.* Ψ_{qp} *is the dihedral angle at the point* ***R***.

Q and ***P*** or by deciding from the direction of conical rotation and so on. If the only one sensor angle α_p is known, the direction of ***R*** is given at many points on a circle of angular radius α_p circumscribing ***P***. Therefore, a single sensor gives no useful attitude solutions in the three-dimensional coordinate system (*e.g.*, SMITH, 1975; SULLIRAN and STICK, 1977). Usually a geomagnetic aspect sensor (GA) has been used which can detect a tip angle α_p and the vector ***P*** corresponds to the geomagnetic field. Sometimes other sensors were used, such as a solar aspect sensor (SS), a moon aspect sensor (MS) and an earth horizon aspect sensor (HOS). The azimuth-elevation coordinate system (X, Y, Z) was frequently used with the origin O corresponding to the launching points. In the case of a large scale rocket or space satellite, an equatorial inertial coordinate system such as the right ascension-declination coordinate system is used (TOHYAMA *et al.*, 1972).

Now the coordinates of $\boldsymbol{P}(\phi_p, \delta_p)$, and $\boldsymbol{Q}(\phi_q, \delta_q)$, where ϕ is the azimuth and δ is the co-latitude in the XYZ coordinate system, are known and the two sensor angles α_p and α_q are measured, then the directions of $\boldsymbol{R}(\phi_r, \delta_r)$ may be expressed as

$$\delta_r = \cos^{-1}(\cos\delta_p \cos\alpha_p + \sin\delta_p \sin\alpha_p \cos\alpha), \tag{1}$$

$$\phi_r = \cos^{-1}\left(\frac{\cos\alpha_p - \cos\delta_p \cos\delta_r}{\sin\delta_p \sin\delta_r}\right) + \phi_p, \tag{2}$$

where angle α is defined as follows:

$$\alpha = \beta \pm \gamma, \tag{3}$$

$$\beta = \cos^{-1}\left(\frac{\cos\delta_q - \cos\delta_p \cos\alpha_{pq}}{\sin\delta_p \sin\alpha_{pq}}\right), \tag{4}$$

$$\gamma=\cos^{-1}\left(\frac{\cos\alpha_q-\cos\alpha_p\cos\alpha_{pq}}{\sin\alpha_p\sin\alpha_{pq}}\right), \tag{5}$$

$$\alpha_{pq}=\cos^{-1}[\cos\delta_p\cos\delta_q+\sin\delta_p\sin\delta_q\cos(\phi_p-\phi_q)], \tag{6}$$

where α_{pq} is the angular distance between $\boldsymbol{P}$ and $\boldsymbol{Q}$ on the celestial sphere. The sensor angles α_p and α_q can be translated into the angles within $\pi/2$ supposing that the vectors replace the direct opposite directions in a sphere when the sensor angles are more than $\pi/2$. In general, the vectors $\boldsymbol{P}$ and $\boldsymbol{Q}$ are located in a hemisphere and the angles α_{pq}, β and γ may take the value within π. From eq. (3), α is two solutions and these are corresponding to the two cones intersecting solutions $\boldsymbol{R}_1$ and $\boldsymbol{R}_2$ in Fig. 1.

2. Geomagnetic Aspect Sensor

The geomagnetic aspect sensor has been used for determination of vehicle attitude since 1962 in Japan and has been aboard most of sounding rockets. At Syowa Station in Antarctica, it have been first used in 1971 and there have been 32 sounding rocket-borne aspect sensors (AOYAMA and TOHYAMA, 1975, 1978; TOHYAMA and AOYAMA, 1978).

The geomagnetic aspect sensor is a fluxgate magnetometer consisting of two component sensors. One of the sensors is mounted in the direction of vehicle axis and the other is mounted in the direction of a plane perpendicular to the vehicle axis (TOHYAMA *et al.*, 1976). Fig. 2 shows a diagram of the aspect sensor system. The main characteristics of the instrumentation are given in Table 1.

If the vehicle is spun around the vehicle axis, that is sensor axis Z_s, the output form of the sensor X_s, perpendicular to Z_s, may be like a sine wave corresponding to the vehicle spin. A maximum value of the sine wave may give a minimum angle

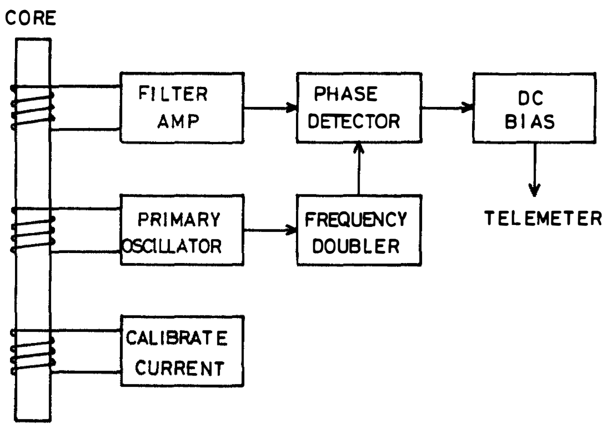

Fig. 2. Schematic system of a geomagnetic aspect sensor (one component).

Table 1. Main characteristics of onboard geomagnetic aspect sensor for antarctic rockets.

Dynamic range	± 50000 nT
Resolution angle	$\pm 1°$
Size	Electronics $95 \times 95 \times 45$ mm^3
	Sensors $41 \times 19 \times 70$ mm^3
Output	DC 0–5 V
Weight	0.6 kg (included sensors)
Power	+18 V 17 mA
	−18 V 10 mA
Drive frequency	22.5 kHz

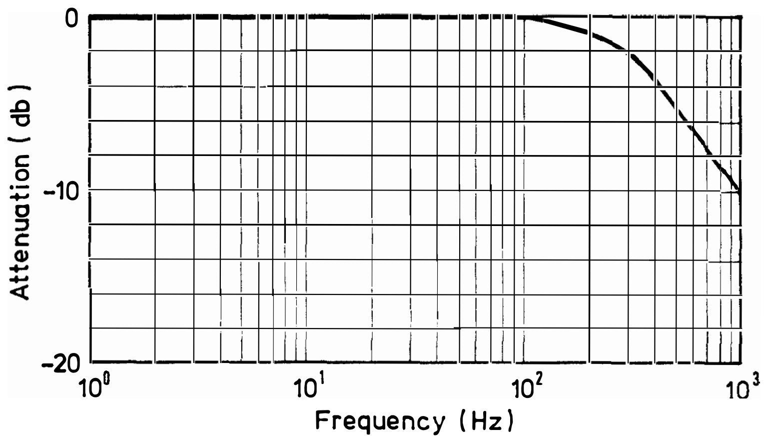

Fig. 3. The property of GA's output voltage attenuation against external magnetic field frequency.

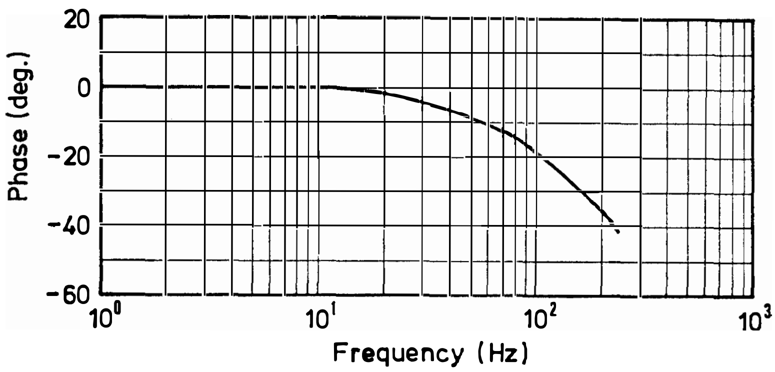

Fig. 4. The property of GA's phase angle delay of output to external ac field.

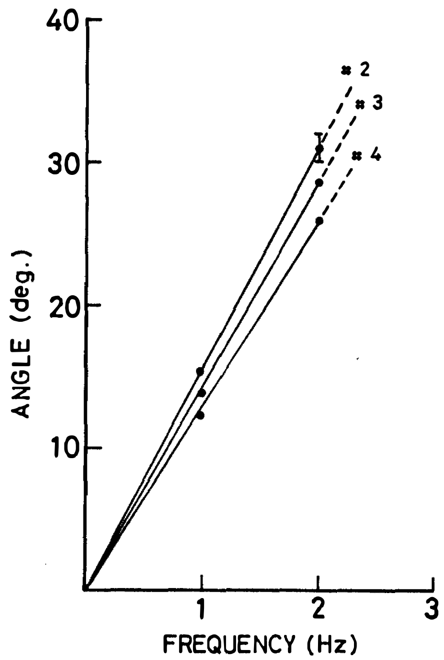

Fig. 5. Delayed phase angle property of the telemeter and discriminator response. It shows the IRIG telemeter channel Nos. 2, 3 and 4 (for the property of S-310JA-7 rocket, March 12, 1978).

between the geomagnetic field vector and the sensor axis X_s. Many physical instruments frequently require the angle information and the time of the minimum angle. However, the phase of the sine wave is delayed by the telemeter circuit systems used.

Fig. 3 shows that sensor output intensity is responsible for external magnetic field frequency. Fig. 4 shows the characteristics of phase delay against ac field. But the phase angle is increasingly delayed by the use of telemeter, for instance, the value is 10°–15° when the spin rate is 1 Hz in case of using the telemeter channel No. 2, 3 and 4 of IRIG, as shown in Fig. 5. Usually the X_s output have used telemeter of channel No. 3 and the spin rate of rockets are 1～2 Hz, so the delay is about 13～28 degrees.

3. Data Analysis for Geomagnetic Aspect Sensor

A vehicle is slowly spun by aerodynamical force to tall planes and the spin rate may be steady for about 50 s after launch. Nose fairings of vehicle are ejected at 55 s after launch and most vehicles start a precessional motion.

Fig. 6 shows a precessional motion on a circle of angular radius α_c circumscribing the center of precession $\boldsymbol{C}$. If the precessional motion is unchanged during the time, $\boldsymbol{C}$ is fixed and α_c and the precessional angular velocity Ω are constant in the inertia coordinate system. Consider the angular distance between $\boldsymbol{C}$ and $\boldsymbol{B}_t$, that is the geomagnetic field vector $\boldsymbol{B}$ at the time t, is θ_{ct}, then the angular distance θ_{rt} from $\boldsymbol{B}_t$ to the rocket axis Z_{rt} is written as

$$\theta_{rt}=\cos^{-1}\left[\cos\theta_{ct}\cos\alpha_c+\sin\theta_{ct}\sin\alpha_c\cos\Omega\,(t-t_0')\right], \tag{7}$$

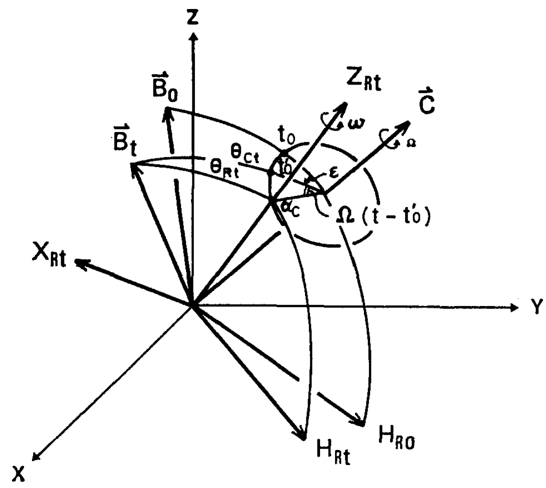

*Fig. 6. Schematic precessional motion in the inertia coordinate system. **C** is the center of precession with the precession velocity Ω and the angular radius α_c. $\boldsymbol{B}_o$ and $\boldsymbol{B}_t$ are the geomagnetic field vectors at the time t_0 and t respectively. Z_{rt} is the orientation of rocket axis at t with the spin velocity ω. X_{rt} is the direction of X sensor that is mouted on the plane perpendicular to Z_r axis, and H_{rt} is the supposed orientation of X axis that is within the meridian of $\boldsymbol{B}_t$ and Z_{rt}. θ_{ct} and θ_{rt} are angles between $\boldsymbol{B}_t$ and **C**, and between $\boldsymbol{B}_t$ and Z_{rt} on the celestial sphere, respectively.*

where t_0' is the supposed passage time at the point Z_{rt_0} which gives a minimum angle of θ_{rt} in Fig. 6. The sensor output intensities X_{rt} and Z_{rt} are given as

$$X_{rt} = B_t \sin\theta_{rt} \cos\omega\,(t-t_0), \tag{8}$$

$$Z_{rt} = B_t \cos\theta_{rt}, \tag{9}$$

where ω is angular velocity of vehicle spin that is unchanged during the time. B_t is the intensity of the geomagnetic field $\boldsymbol{B}_t$. But the B_t is different from the vector $\boldsymbol{B}_{t_0}$ at the time t_0, the angle of $\Omega(t-t_0)$ has ambiguous angle ε (Fig. 6). Consider the angular distance between $\boldsymbol{B}_0$ and $\boldsymbol{B}_t$ is α_b, the angle ε is given as

$$\varepsilon = \cos^{-1}\left(\frac{\cos\alpha_b - \cos\theta_{co}\cos\theta_{ct}}{\sin\theta_{co}\sin\theta_{ct}}\right), \tag{10}$$

$$\Omega(t-t_0') = \Omega(t-t_0) - \varepsilon, \tag{11}$$

where t_0 is the time of giving a minimum angle of θ_r during the precession from the data. As the spin velocity ω is usually large than the precession velocity Ω and the ratio of Ω/ω is $\lesssim 10^{-2}$, it is difficult to fix the accurate time of t_0 from the data. The sensor axis X_s is spun with the angular velocity ω and the output form may depend on cos ωt. It is difficult to resolve the epoch time of cos ωt. If the epoch time can be defined when the sensor axis points to the direction of H_{ro} that is within the plane of $\boldsymbol{B}_t - Z_{rt}$ meridian in Fig. 6, then the output of X_{rt} is given by eq. (8). Accordingly an observed spin rate from data of X_{rt} is based on the vector $\boldsymbol{B}_t$, the apparent spin rate may be changeable even if the rate is constant in the inertia coordinate system. The true spin rate is computed from an average of one precessional motion if the direction of vector $\boldsymbol{B}$ is not changed during the period. Actually the theoretical changes of the geomagnetic field during one precessional motion are about 1.3 degrees in the case of antarctic sounding rockets, so an average value of ε of eq. (10) is $\sim$2.5° and an average apparent change of spin rate during one precession is $\sim 2 \times 10^{-3}$ Hz, that is equivalent to the phase angle ambiguity of 0.5 degrees/spin. For this reason, we may use the first ordered assumption that the vector $\boldsymbol{B}$ is fixed during a flight with the azimuth-elevation coordinate system (X, Y, Z) and its origin O is corresponding to the launch site and also we may use the theoretical $\boldsymbol{B}$ at the launching time. As the maximum output of X_{rt} that is conform to the direction of H_{rt} is given by the data, the X_{rt} is equal to $B_t \sin\theta_{rt}$ from eq. (8). At this time, the angular distance from $\boldsymbol{B}_t$ to the rocket axis is given as

$$\theta_{rt} = \tan^{-1}\left(\frac{H_{rt}}{Z_{rt}}\right), \tag{12}$$

and θ_{rt} is independent of the intensity B at any time in flight. H_{rt} and θ_{rt} can be obtained at every spin period.

From eqs. (7), (8) and (9), the sensor output forms of X_r and Z_r are as shown in Fig. 7. Fig. 7a is typical output in the case of precessional motion that is modulated from precession angle and period. Fig. 7b is an output in the case of no precession and unchanged attitude in space, or in a special case where the vector $\boldsymbol{C}$ coincides with the vector $\boldsymbol{B}$. Although the maximum angle θ_{rM} and the minimum angle θ_{rm} of θ_r are known from the data like Fig. 7 and from eq. (12), the peak-to-peak angle is not always equal to $(\theta_{rM} - \theta_{rm})$. The reason is that the coning full angle is equal to $(\theta_{rM} + \theta_{rm})$ when the vector $\boldsymbol{B}$ is included in the cone of precession. There-

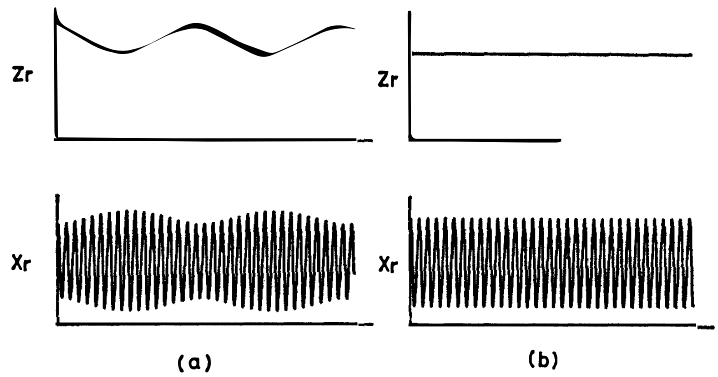

Fig. 7. Typical output analog form of GA during precessional motion (a) and stable motion (b). The longitudinal axis is output voltage and the sidelong axis is time in each figure.

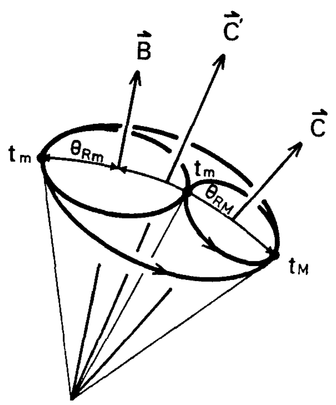

*Fig. 8. Two cones of precession. Both cones give the same minimum angle θ_{rm} and the same maximum angle θ_{rM} from **B**.*

fore, two centers of precession, $\boldsymbol{C}$ and $\boldsymbol{C}'$ are considerable as shown in Fig. 8. In the case of $\boldsymbol{C}$, θ_c is equal to $(\theta_{rM}+\theta_{rm})/2$ and α_c is equal to $(\theta_{rM}-\theta_{rm})/2$ and $\theta_c>\alpha_c$. In the case of taking $\boldsymbol{C}'$, the value of θ_c and α_c is inversed relation to that of $\boldsymbol{C}$ respectively. It is difficult to distinguish between $\boldsymbol{C}$ and $\boldsymbol{C}'$ without the use of another aspect sensor.

4. Other Aspect Sensors

The geomagnetic aspect sensors have been boarded on all Antarctic sounding rockets, and at the same time six solar aspect sensors, four moon aspect sensors and two horizon aspect sensors have used during the IMS period.

The solar aspect sensor is analog type detector which measures the light position through the sensor slit. A potentiometric resistor made of CdS is used and the angle resolution is $\pm 1°$ and the range of angle is 120° in the incident meridian.

The moon aspect sensor is like a phototube which can detect weak moon light. Especially in Antarctica, many sounding rockets were launched to observe auroral physical phenomena at night, and the use of the moon aspect sensor is convenient for attitude determination. The investigator of the attitude determination by the moon sensor was the Geophysical Research Laboratory, University of Tokyo.

The horizon aspect sensor consists of a telescope with a narrow field of view, that contains a sensing element to detect the change in visible light intensity between the sunlit earth and the space or between the sunlit earth and the shadowed earth. The investigator of the attitude determination by the horizon sensor is the Faculty of Engineering, Kobe University.

Sometimes it is difficult to detect a sensor angle with a sun aspect sensor or a moon aspect sensor. The reason is that the resolution of angle falls owing to large albedo of antarctic ice when the sun and the moon are seen close to the horizon.

5. Summary Results of Antarctic Rocket Attitudes

5.1. Spin property

The vehicle spin properties of the IMS antarctic sounding rockets are shown in Fig. 9. The time dependency of the spin rate for S-210 type rockets and that for S-310 type rockets are shown in Figs. 9a and 9b respectively. The same type vehicles show similar profiles except two rockets, S-210JA-30 and -31 which the spin of vehicles stopped by despin motors. About S-210 type vehicles, the spin frequency has the value of 1.80~2.50 Hz, the average being 2.1 Hz. Spin profiles of the S-310 type vehicles show that the rate goes down at about 50 s after launch by yo-yo despiners and then takes a constant frequency of 0.71~1.05 Hz. The average spin frequency is 0.94 Hz.

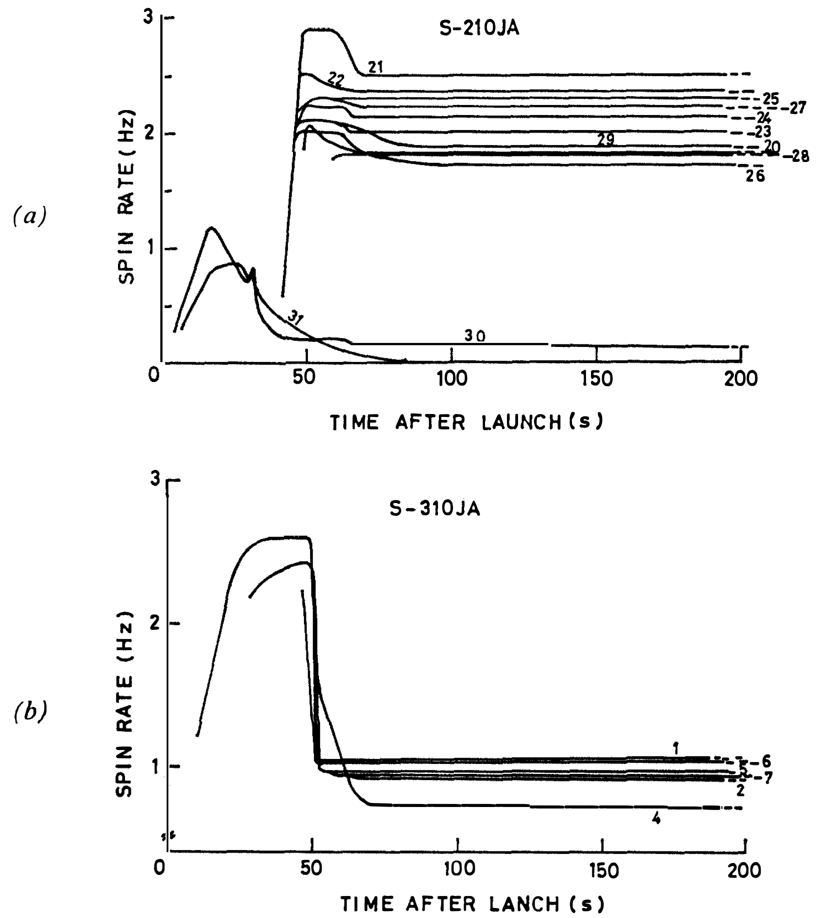

Fig. 9. Summary spin frequency profiles during flight of S-210 type vehicles (a) and that of S-310 type vehicles (b).

5.2. Precession property

Before the time of the nose fairing separation at about 55 s after launch, the direction of vehicle axis changes slowly by aerodynamic force. Some S-210 type vehicles show unstable aspects before the seperation, especially in the case of vehicle having lower spin. After the nose fairing taking off, most vehicles show precessional motions. The sensor angles between the vehicle axis and the theoretical geomagnetic field at Syowa Station are shown in Figs. 10a and 10b. The theoretical geomagnetic field is computed by a spherical harmonic expansion using the 1975.0 IGRF coefficients, for instance the total intensity, the declination and the inclination are 45640 nT, $-46°.53$ and $-65°.08$ respectively at the time of 1976.71 (TOHYAMA and ONISHI, 1977).

There are three species of precession profiles for S-210 type vehicles;

(1) the precessional angle is relatively small ($\lesssim 20°$) and the long precession period ($\gtrsim 70$ s); (S-210JA-20, -21, -23, -24 and -25),

(2) the precessional angle is large ($\gtrsim 30°$) and the short precession period ($\lesssim 60$ s); (S-210JA-28, -29, -30 and -31),

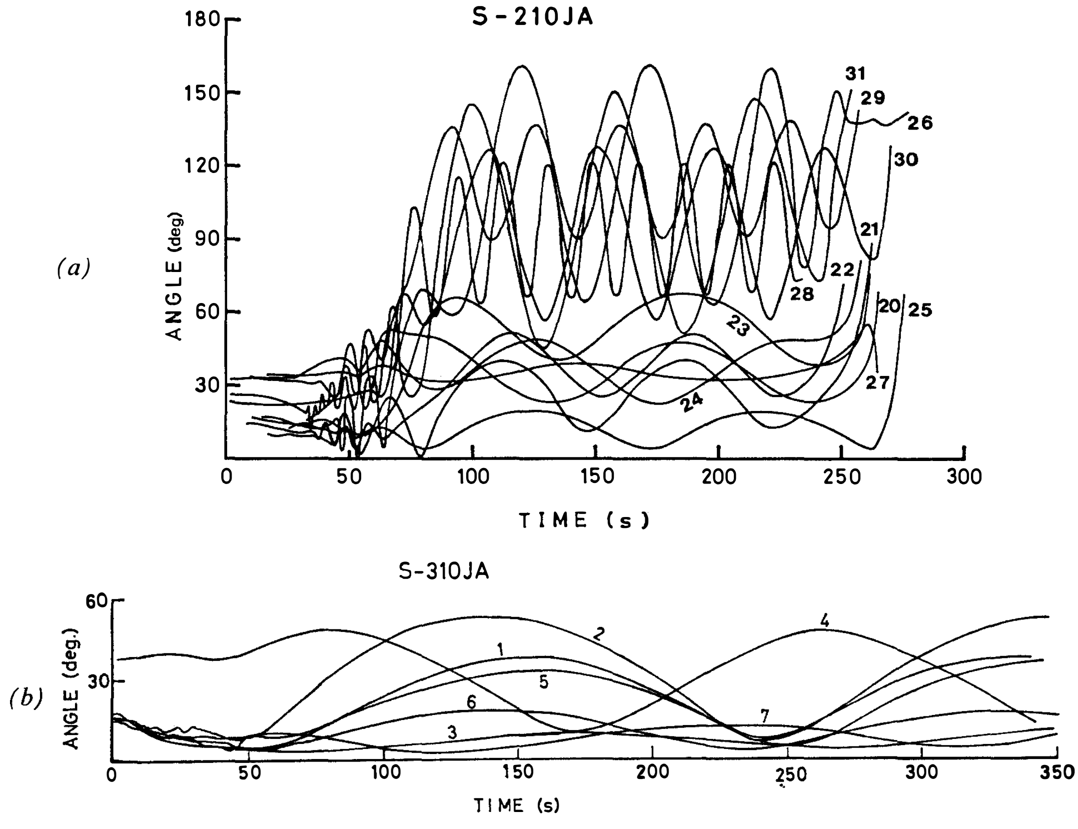

Fig. 10. Summary aspect angles during flight between the rocket axis and the theoretical geomagnetic field at Syowa Station. The numeral is the rocket number of S-210 type (a) and S-310 type (b) vehicles.

Table 2. Summary attitude results.

Rocket	Launching Date	Launching Time	Launching Azimuth (Deg.)	Spin Freq. (Hz)	Precession Angle (Deg.)	Precession Period (s)	Remarks
S-210JA-20	June 25, '76	0240	135	1.82	12	108	
21	July 26	0323	315	2.50	14	76	
22*	Jan. 26	0220	315	2.36	39**	74	SS
23	Sep. 13	0731	315	2.00	13	100	
24*	Aug. 17	0254	135	2.12	13	96	MS
25*	Sep. 1	0300	315	2.27	8	95	MS
26*	Apr. 11, '77	0800	246	1.80	49	52	SS
27*	Aug. 10	1547	135	2.21	36**	110	SS
28*	Mar. 27	0655	264	1.80	87**	18	SS
29	July 12	1915	315	1.85	67**	35	MS
30*	Jan. 28, '78	2310	22	0.17	35	45	SS
31*	Feb. 6	2155	39	0	54	57	SS
S-310JA-1	Feb. 13, '76	1245	315	1.05	15	180	
2	Feb. 10, '77	0322	315	0.89	24	200	
3*	July 26	1835	315	0.96	6	220	MS
4*	Aug. 18, '78	0332	130	0.71	19	185	HOS
5*	June 11	0156	315	0.96	15	195	HOS
6	Aug. 28	0056	315	1.02	7	186	
7	Mar. 27	2215	315	0.91	5	178	

The launching time is local time at Syowa Station (45° EST), the azimuth from the north. SS, MS and HOS in the remarks section mean to be onboarded together with GA, they are solar aspect sensor, moon aspect sensor and horizon aspect sensor respectively. The rocket of determinating absolute attitude is shown as asterisk * and the precessional cone included the field or the sun is shown as double asterisk **.

(3) the intermediate property of (1) and (2); (S-210JA-22 and -27).

The average precessional angle is about 32 degrees and the period is about 72 s except S-210JA-30 and -31 rockets. The attitudes of S-310 type vehicles are relatively stable and the precessional angle is 5～24 degrees and the period is 200 ± 20 s. The average precessional angle and period are 13 degrees and 192 s respectively.

Table 2 shows the attitude characteristics of the antarctic sounding rockets during the IMS period (1976–1978), launched at Syowa Station, Antarctica.

5.3. Absolute attitudes

The three-dimensional attitudes of 11 vehicles are determined by using two aspect sensors (Table 2). Fig. 11 shows the orientation of the vehicle axis in the azimuth-elevation coordinate system. It is found S-310 type vehicles and S-210JA-24 and -25 show stable attitudes of flight. S-210JA-26, -28 and -31 rockets show large

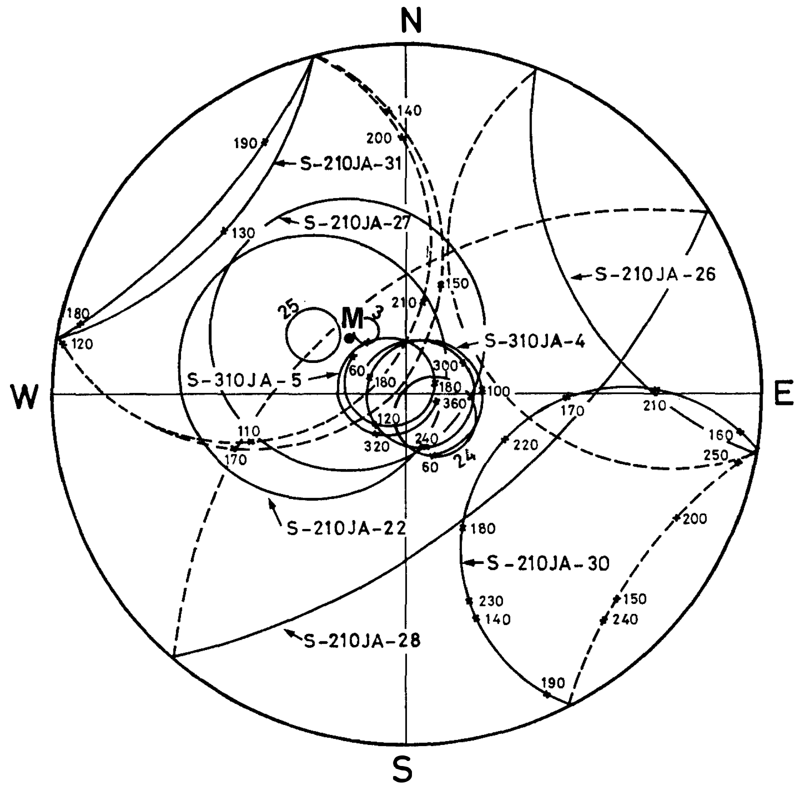

Fig. 11. Summary absolute attitudes in the stereographic projection, Wulf net that the center point is corresponding to the zenith and the circumference is applicable to the horizon at Syowa Station.

precession and S-210JA-22 and -27 rockets show average precession. The absolute attitudes of other rockets are not determined because of the use of the single aspect sensor or noisy aspect data.

6. Discussion

One of the problems for the attitude determination is that an absolute direction cannot be determined by the single aspect sensor because of the spin stabilized vehicle. Sometimes two aspect sensors are not put onboard a vehicle for the reason of no room and over-weight. If a phase angle Ψ_{qp} between the reference vector $\boldsymbol{Q}$ and the vector $\boldsymbol{P}$ (Fig. 1) is detectable, the direction $\boldsymbol{R}$ may be determined. Then it is easy to improve the geomagnetic aspect sensor equipped with a solar cell and a phase angle counter.

The second problem is to distinguish between $\boldsymbol{C}$ and $\boldsymbol{C'}$ in Fig. 8. We propose here two methods for the distinction. One of them is the spin phase method. If it is able to decide the times of t_M and t_m, ($t_M < t_m$), corresponding to the maximum sensor angle θ_{rM} and the minimum sensor angle θ_{rm} respectively, the spin phase Ψ_{rM} at the time of t_M and Ψ_{rm} at that of t_m are measured from the output of X_{rt} and the relation is given as

$$\Psi_{rm}=\Psi_{rM}+\frac{\tau_c}{\tau_s}\pi. \tag{13}$$

This is an equation when the cone of precessional motion is not included with the vector $\boldsymbol{B}$. Here τ_c and τ_s are the periods of precession and spin respectively. The relation for $\boldsymbol{C}'$ when the cone of precession is included the vector $\boldsymbol{B}$ is given as

$$\Psi'_{rm}=\Psi_{rM}+\left(\frac{\tau_c}{\tau_s}+1\right)\pi. \tag{14}$$

If the spin rate is constant, the phase difference between Ψ_{rm} and Ψ'_{rm} is π.

Another method is to distinguish between $\boldsymbol{C}$ and $\boldsymbol{C}'$ from the value of spin velocity and precessional angle and period. Spin stabilized vehicle is assumed to have symmetry about the principal axis z, so that the moments of inertia about the x and y axes that are perpendicular to z are equal, $I_x=I_y$. If the vehicle axis coincides with a principal axis of inertia, the precession velocity Ω is proportional to the spin velocity ω and it is given as

$$\Omega=\frac{I_z\omega}{(I_x-I_z)\cos\theta}, \tag{15}$$

where θ is corresponding to the angle α_c between the vehicle axis and the precessional axis. Spinning vehicles tend to have $I_x>I_z$, so the directions of the spin and precession are the same from eq. (15) that is known as *direct precession* (Ball and Osborne, 1967). Actually the values of I_z and I_x are 0.13 kgms^2 and 31 kgms^2 respectively for S-210 type vehicles, so that the ratio of $I_z/(I_x-I_z)$ is $4.19\sim4.42\times10^{-3}$, and that for S-310 type vehicles is $4.45\sim5.05\times10^{-3}$. From these ratios and the spin velocity and the precession velocity, α_c may be surmised using eq. (15) and the coning axis may be distinguished either as $\boldsymbol{C}$ or $\boldsymbol{C}'$. For instance, the maximum and the minimum angles for the vector $\boldsymbol{B}$ are 136° and 90° for the S-210JA-29 rocket, so the precession angles are supposed to have two values, 23° and 67°. The former ratio of $I_z/(I_x-I_z)$ is 14.22×10^{-3} and the latter of that is 6.03×10^{-3} respectively, so it seems the precessional angle is 67 degrees, which the vector $\boldsymbol{B}$ is included within the precessional cone. However, it is not useful for the case when two supposed angles are not different enough, *i.e.*, S-310JA-1, -2, -6 and -7 rockets. Also the ratio is not suitable for non-spin vehicles, *i.e.*, S-210JA-30 and -31 rockets.

The third problem is a correction of data. Magnetic offset at the sensor position from the rocket body and physical instruments is usually large. There are mainly dc magnetic bias and shielding effects. The correction is made by using a theoretical value of the geomagnetic field and the calibration before the launch.

Cancel current is used and the sensor location is changed when dc offset is large and when output voltage has not linearity. In any case, it is very important to demagnetize the rocket body and instrumental parts.

Acknowledgments

The authors' thanks are due to the members of the 17th, 18th and 19th Japanese Antarctic Research Expeditions for their efforts in making the rocket launch, the telemetry data aquisition and ground-based observations. These experiments were made as one of the IMS projects of the National Institute of Polar Research and the authors are grateful for the opportunity given them to conduct the experiments.

Thanks are extended to the researchers at the Goephysical Research Laboratory, University of Tokyo for providing the moon aspect data, and to the researchers at the Faculty of Engineering of Kobe University for providing the horizon aspect data. The authors also would like to thank Mr. H. YAMAGISHI of the National Institute of Polar Research for providing the telemetry phase delay data, and to thank Mr. IKUTA of Nissan Motors Co. Ltd. for the inertia moment data of rockets. Sokkisha Co. Ltd. is also acknowledged for the fabrication of rocket-borne geomagnetic aspect sensors and solar aspect sensors.

References

AOYAMA, I. and TOHYAMA, F. (1975): Study of the attitudes of rockets launched at Syowa Station. Nankyoku Shiryô (Antarct. Rec.), **52**, 156–159.

AOYAMA, I. and TOHYAMA, F. (1980): Nankyoku roketto no shisei (Study of the attitudes of rockets launched at Syowa Station). Nankyoku Shiryô (Antarct. Rec.), **68**, 122–128.

BALL, K. J. and OSBORNE, G. F. (1967): Space Vehicle Dynamics. Oxford, Oxford Univ. Press, 135 p.

SMITH, G. A. (1975): Four Methods of Attitude Determination for Spin-Stabilized Spacecraft with Applications and Comparative Results. NASA-Goddard Space Flight Center Document.

SULLIRAN, B. F. and STICK, M. E. (1977): Special utilization of triaxial magnetometer measurements as prime attitude determination sensors. J. Spacecr., **14**, 231–235.

TOHYAMA, F. and AOYAMA, I. (1978): Attitudes of the antarctic sounding rocket vehicles. Mem. Natl Inst. Polar Res., Spec. Issue, **9**, 87–91.

TOHYAMA, F. and ONISHI, N. (1977): Chijiki shisei-kei no tameno jiba keisan (Geomagnetic field analysis for a geomagnetic aspect sensor). Tokai Daigaku Kiyô Kôgakubu (Proc. Fac. Eng., Tokai Univ.), **1**, 241–249.

TOHYAMA, F., AOYAMA, I. and TAKAHASHI, T. (1972): Chijiki shisei-kei ni yoru *Tansei* no shisei sokutei (*Tansei* attitude measurement by magnetometers and sun sensor). Tokyo Daigaku Uchû Kôkû Kenkyûjo Hôkoku (Bull. Inst. Space Aeronaut. Sci., Univ. of Tokyo), **8**, 121–129.

TOHYAMA, F., ONISHI, N. and MIYAZAKI, M. (1976): *K-10-11 goki* chijiki shisei-kei (Geomagnetic aspect sensors of *K-10-11* rocket). Tokyo Daigaku Uchû Kôkû Kenkyûjo Hôkoku (Bull. Inst. Space Aeronaut. Sci., Univ. of Tokyo), **12**, 1000–1003.

(Received July 25, 1980)